

Reassignment of the 11 537 cm⁻¹ Band of Hydrogen Fluoride Dimer and Observation of the Intermolecular Combination Mode 3ν₁ + ν₄

Cheng-Chi Chuang, Susy N. Tsang, and William Klemperer*

Department of Chemistry, Harvard University, Cambridge, Massachusetts 02138

Huan-Cheng Chang

Institute of Atomic and Molecular Sciences, Academia Sinica, P. O. Box 23-166, Taipei, Taiwan 10764, Republic of China

Received: March 6, 1997; In Final Form: April 23, 1997[⊗]

We reexamine the $N = 3$ valence excitations of (HF)₂ and their combinations with intermolecular vibrations using a high-sensitivity germanium detector which collects the first overtone emission of fragment HF. We use the specific vibrational product state production to assign the quantum numbers within a vibrational polyad. The band previously assigned to $K = 1$ of $\nu_1 + 2\nu_2$ (*J. Chem. Phys.* **1994**, *100*, 1) is shown to originate from $K = 1$ of $3\nu_2 + \nu_6$. This assignment, based on photofragment HF vibrational state, is supported by the observation of quenched hydrogen interchange tunneling ($\Delta\nu_t = -0.6$ GHz) and rapid vibrational predissociation [$\Delta\nu_{pd} = 3.5(10)$ GHz] of this state. The $K = 1$ band origin of the lower A⁻ level is 11 537.047(6) cm⁻¹. The rotational constants for the two tunneling components are the same within experimental error, (\bar{B}) = 0.2182(2) cm⁻¹. The out-of-plane vibration frequency, $3\nu_2 + \nu_6 - 3\nu_2 = 493.96(3)$ cm⁻¹, is increased 25% from the ground state. The predissociation rate of this combination state is a factor of three slower than that observed at $3\nu_2$. The combination mode $3\nu_1 + \nu_4$ has band origins of $\nu_0 = 11\ 402.889(4)$ and $11\ 402.867(8)$ cm⁻¹ and rotational constants of $\bar{B} = 0.216\ 39(17)$ and $0.217\ 04(15)$ cm⁻¹ for the two tunneling components A⁺ and B⁺, respectively. The tunnel splitting $\Delta\nu_t = \nu_0(\text{B}^+) - \nu_0(\text{A}^+) = -0.021(8)$ cm⁻¹. The frequency of ν_4 the intermolecular or hydrogen bond stretching vibration, $3\nu_1 + \nu_4 - 3\nu_1 = 129.36$ cm⁻¹, is quite similar to that at ν_1 , suggesting only a minor dependence of the hydrogen bond vibration on the free-HF bond length. The $3\nu_1 + \nu_4$ band has a predissociation linewidth of 2.5(2) GHz, one order of magnitude larger than the 0.24(2) GHz of the pure overtone $3\nu_1$ state. The coupling of this level to the dark state $3\nu_2 + \nu_4 + \nu_5$ is suggested as the origin of the observed linewidth increase.

Introduction

For many decades the hydrogen fluoride dimer has served, and continues to serve, as a model system for understanding intermolecular interactions in general, and hydrogen bonding specifically, of molecular complexes. The relative ease of its preparation and its spectral simplicity have permitted a broad variety of detailed spectroscopic studies.¹ These spectroscopic studies have generally focused upon the structural and dynamical properties of the complex and are frequently discussed by means of an increasingly sophisticated multidimensional quantum dynamical treatment. While direct absorption² and optothermal³ measurements are providing massive information for lower vibrational levels, the ease of observing infrared laser-induced fluorescence⁴ ensures that increasingly energetic states of the ground electronic potential surface can be characterized in a detailed manner.

The hydrogen fluoride dimer may superficially appear as a simple hydrogen-bonded system; however, because it contains two identical units, there are frequently bizarre behaviors. It is certainly a much more complicated system than ArHF or N₂HF, both of which have provided considerable insight into the nature of hydrogen bonding. Despite six-dimensional (6D) quantum dynamical calculations having been made for this prototypical complex,⁵ it remains worthwhile to discuss features in terms of simple physical constructs. In the present work we continue to emphasize excitations in the region of three quantum valence

vibrations of the two HF subunits, i.e., the $N = \nu_1 + \nu_2 = 3$ polyad. Studies in this region yield important information about the potential energy surface (PES) of the hydrogen bond, since the valence coordinates of both the proton donor and also the acceptor experience average extensions by up to 10% from the equilibrium value. In addition to the PES, the studies also probe predissociation and hydrogen interchange tunneling dynamics at higher vibrational energies, where the density of states has become extremely high.

The relation between dimeric behavior and the collisions of hydrogen fluoride has not been a topic of emphasis of recent research.⁶ It, however, is worth noting that, at $N > 1$, phenomena closely akin to V–V vibrational energy transfer in the collision of HF(ν) + HF(ν') = HF($\nu + 1$) + HF($\nu' - 1$) appear in the spectra of (HF)₂. The dimeric analogue of this collisional process does not lead to line broadening by predissociation as it does in the analogue of HF(ν) + N₂(ν') = HF($\nu - 1$) + N₂($\nu' + 1$), found in the analysis of the photofragmentation spectrum of N₂HF,⁷ because of small energy release. The features in the (HF)₂ spectrum that are analogous to V–RT (vibration to rotation and translation) relaxation are primarily the predissociation linewidths. That predissociation of hydrogen-bonded complexes is interesting is readily seen from its dependence upon valence bond excitation. In (HF)₂, the ratio of linewidths in the (ν_1, ν_2) = (0,3) band compared to those in (0,1) is 30.¹ In N₂HF, the predissociation linewidth is 7.2 MHz at $\nu_{\text{HF}} = 1$,⁸ 79 MHz at $\nu_{\text{HF}} = 2$,⁹ and 580 MHz at $\nu_{\text{HF}} = 3$,¹⁰ respectively. Thus the rate of predissociation of the

[⊗] Abstract published in *Advance ACS Abstracts*, August 1, 1997.

directly hydrogen-bonded HF unit appears to scale between ν_{HF}^3 and ν_{HF}^4 . The origin of this strong vibrational dependence is of interest. The obvious explanation is that the increase in the rate of predissociation is a consequence of the rapid increase of level density with energy; however, we will show that this explanation is unlikely.

We have previously^{11,12} presented the data for the 11 000–11 500 cm⁻¹ absorption features of the hydrogen fluoride dimer, obtained by using an infrared laser-induced fluorescence technique. The present work is primarily a reinvestigation of the vibrational assignments in the energy region of the $N = 3$ vibrational polyad. The vibrational assignments in the (HF)₂ spectrum have been based upon several characteristics of the bands: (a) the stretching frequencies, (b) the transition intensities, (c) the rotational structures, and (d) the predissociation linewidths. Of the four bands observed, the narrowest linewidth is that in (3,0), FWHM = 240 MHz,¹³ corresponding to a predissociation time of 660 ps. This establishes that many features in the (HF)₂ spectrum can be detected by monitoring the photofragmentation product HF emission. We shall exploit the spectral character of this emission to aid the vibrational assignment of the (HF)₂ excitation spectrum.

Four bands were suggested as comprising the $N = 3$ quartet of (HF)₂ in the frequency region between 11 000 and 11 500 cm⁻¹.¹² In the earlier experiments,¹⁴ the detection of fluorescence was achieved by using a lead sulfide detector cooled to 240 K. This detector measures radiation near 3500 cm⁻¹, corresponding to the $\Delta\nu = -1$ emission of HF monomer. Our primary concern here is the vibrational assignment of the weakest component of the quartet at 11 537 cm⁻¹. It was assigned as the $K = 1 \leftarrow 0$ subband of $\nu_1 + 2\nu_2$. In modeling the static and dynamical properties of the valence excitations of (HF)₂,¹⁵ this assignment was quite discordant. In particular, the feature is 50 cm⁻¹ lower in frequency than expected on the basis of a coupled local oscillator model. Additionally, only the $K = 1 \leftarrow 0$ subband was observed, whereas the $K = 0 \leftarrow 0$ subbands are the most intense for the other three members of the quartet. Furthermore, the tunneling splitting ($\Delta\nu_t$) was observed to be negligible, while the $\Delta\nu_t$ in the $2\nu_1 + \nu_2$ band is large. Modeling the tunneling led to the expectation that the magnitude of the splittings in the $\nu_1 + 2\nu_2$ and $2\nu_1 + \nu_2$ levels would be quite similar,¹⁵ as indeed the tunneling splittings are in the ν_1 and ν_2 levels.

This paper deals with the reexamination of the laser-induced fluorescence of the 11 537 cm⁻¹ feature using a high sensitivity germanium detector, which is sensitive to radiation with energy greater than 6300 cm⁻¹. The radiation can only be produced by $\Delta\nu = -2$ overtone transitions of HF photofragments. While our earlier work,¹² using a lead sulfide detector, did not permit the vibrational states of the products to be analyzed, we will show that the additional detection of $\Delta\nu = -2$ emission provides diagnostically valuable product state discrimination. In addition to this band, new features recorded around 11 402 cm⁻¹ will also be reported. The assignment of these two bands at 11 402 and 11 537 cm⁻¹ to the combinations of valence stretching with the two low-frequency intermolecular vibrations, ν_4 (van der Waals stretch) and ν_6 (out-of-plane torsion), will be discussed.

Experimental Section

The major features of the apparatus have been described previously.^{11,14} The substantive changes are the incorporation of a highly stable amplitude-modulated argon ion laser (Coherent) for pumping the titanium sapphire crystal. By employing an acoustooptic modulator (IntraAction Corp.),¹⁶ up to 90% modulation of the single-mode titanium sapphire laser power

could be achieved without notable deterioration of frequency stability. With this new amplitude modulation (AM) scheme, a laser linewidth of 10 MHz could be maintained. The narrow laser bandwidth allows the predissociation lifetime of the sharpest rovibrational features of the $3\nu_1$ band to be precisely determined. The typical intracavity amplitude-modulated power is estimated at about 30 W, corresponding to an intensity of 10³ W cm⁻².

In the present experiment, we monitor the first overtone fluorescence of the HF fragments at $(7-8) \times 10^3$ cm⁻¹, with the excitation of (HF)₂ at $(11-12) \times 10^3$ cm⁻¹. The fluorescence is collected outside the slit jet chamber using $f/1$ lenses and a liquid-nitrogen-cooled germanium detector (Applied Detector Corp.),¹⁷ which has a noise-equivalent power of 10⁻¹⁴ WHz^{-1/2} and a long wavelength cutoff of 1.6 μm . The ultrahigh sensitivity of the detector compensates for the low collection efficiency (<0.001%) of total emission, due to the long radiative lifetime (>3 ms) of HF stretching,¹⁸ the small fraction of overtone emission, and the high translational velocity (5×10^4 cm/s) of the supersonically expanded molecules. While the fluorescence is emitted at a frequency remote from the excitation, it was found that simple bandpass filtering is quite inadequate when using AM. A considerable effort was thus expended to reduce scattered laser radiation. The laser is also capable of being operated in frequency modulation mode, with appreciable reduction in amplitude-modulated scattered radiation. The modulation depth in FM is usually 30–100 MHz, less than a cavity mode spacing. FM is quite ineffective for detecting broad features with linewidths greater than 1 GHz.

Results and Analysis

We have reexamined the spectrum of the $N = 3$ quartet of (HF)₂ previously reported.¹² The previously observed and securely assigned features at 11 043 cm⁻¹ ($3\nu_2$), 11 273 cm⁻¹ ($3\nu_1$), and 11 552 cm⁻¹ ($2\nu_1 + \nu_2$) are readily observed with the Ge detector, which gives threefold improvement in the signal-to-noise (S/N) ratio. In addition to these three bands, combination bands of $3\nu_2 + \nu_6$ (centered at 11 537 cm⁻¹) and $3\nu_1 + \nu_4$ (centered at 11 402 cm⁻¹), are recorded with the present frequency-stabilized amplitude modulation and $\Delta\nu = -2$ fluorescence detection scheme.

A. The $K = 1 \leftarrow 0$ Subband of $3\nu_2 + \nu_6$. The action spectrum of the $K = 1 \leftarrow 0$ subband of $3\nu_2 + \nu_6$ is shown in Figure 1. It should be noted that the central portion of this spectrum is virtually identical to that of Figure 2 in ref 12. The only difference is that the present spectrum is recorded by detecting $\Delta\nu = -2$ fluorescence and exciting with a laser linewidth of 10 MHz, instead of detecting $\Delta\nu = -1$ and exciting with a 180 MHz laser linewidth as used previously. The spectrum shows the characteristics of a perpendicular transition, $K = 1 \leftarrow 0$, notably the two prominent Q branches arising from the two tunneling components, A⁺ and B⁺.¹² Due to extensive line broadening from efficient vibrational predissociation, the transitions of the weaker P and R branches could only be observed with difficulty. A considerable effort has been expended to obtain rotationally resolved structures within the R branches. The structured features in Figure 1 are assigned to $R(2) - R(7)$ of A⁻ \leftarrow A⁺ and $R(1) - R(6)$ of B⁻ \leftarrow B⁺. Each of these branches is fit with a band origin and a rotational constant, B_{eff} , using the standard slightly asymmetric prolate rotor energy expression, where we have incorporated the effects of asymmetry in the $K = 1$ level into B_{eff} (the centrifugal distortion is set at the ground state value of 2×10^{-6} cm⁻¹). The fitting constants for the A⁻ \leftarrow A⁺ R branch are $\nu_o = 11 537.047(5)$ cm⁻¹ and $B_{\text{eff}} = 0.21 616(21)$ cm⁻¹. The fitting

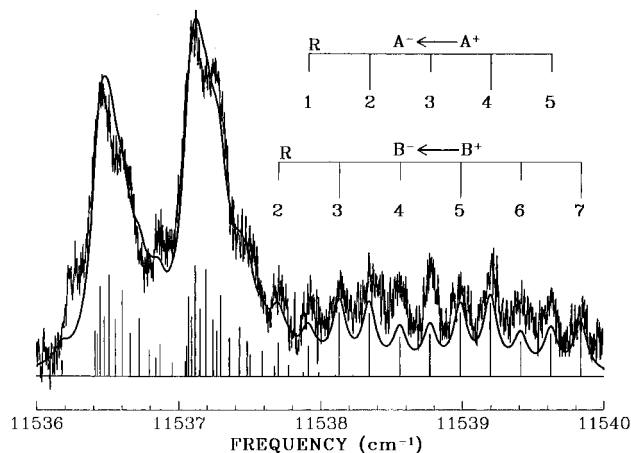


Figure 1. $K = 1 \leftarrow 0$ subband of the $3\nu_2 + \nu_6$ mode of $(\text{HF})_2$. The spectrum was taken by detecting the first overtone fluorescence of HF fragments by using a liquid-nitrogen-cooled Ge detector, with the intracavity laser power of 30 W and a time constant of 3 s. The prominent features are the two Q branches arising from hydrogen interchange tunneling between the two HF subunits. The simulated spectrum shown underneath is generated by using a temperature of 15 K, band origin of $11\,537.047\text{ cm}^{-1}$ ($11\,536.406\text{ cm}^{-1}$), and rotational constant $F(B + C, 2) = 0.218\,16$ ($0.218\,23$) cm^{-1} , for the $A^- \leftarrow A^+$ ($B^- \leftarrow B^+$) transition. Common constants for both bands are asymmetry $B-C = 0.008\text{ cm}^{-1}$, centrifugal constant $D_J = 2 \times 10^{-6}\text{ cm}^{-1}$, and Lorentzian width of 3.5 GHz. The calculated locations of individual lines are shown at the bottom of the figure. The assignments of the resolved features of the R branches are shown for the two bands.

constants for the $B^- \leftarrow B^+$ R branch are $\nu_o = 11\,536.406(7)\text{ cm}^{-1}$ and $B_{\text{eff}} = 0.216\,23(21)\text{ cm}^{-1}$. These constants fit the measured lines within experimental uncertainty. The maximum difference between observation and experiment is 0.008 cm^{-1} ; therefore we do not list the frequencies of these distinct features. The final important parameter is the Lorentzian component, Γ_L , of the Voigt profile. A best fit, $\Gamma_L = 3.5 \pm 1.0\text{ GHz}$, is obtained with broad error limits by visual comparison of several calculated spectra with the observed. The Doppler linewidth of $(\text{HF})_2$ is constrained to 180 MHz, which is $(3/2)^{1/2}$ times the linewidth observed for ArHF, 145 MHz. ArHF has a negligibly small predissociation linewidth ($\approx 30\text{ kHz}$).

From the band origins and the known inversion splitting of the ground state the tunnel splitting in this state is $\Delta_t = -0.018(9)\text{ cm}^{-1}$. The two distinct Q branches are then fit with the rotational constants B_{eff} increased by 0.004 cm^{-1} from their values obtained from the fit of the R branches. The value 0.004 cm^{-1} is the estimate for the asymmetry or l doubling of the $3\nu_2 + \nu_6$ state. This single parameter was adjusted to reproduce the overall appearance of the Q branches. The stronger band is the transition of $A^- \leftarrow A^+$, since the A^+ level at the ground vibrational state is significantly more ($\approx 10\%$) thermally populated than B^+ at the jet temperature of 15 K. The weaker feature is the transition $B^- \leftarrow B^+$. The threefold reduction in the Lorentzian linewidth, 3.5 (10) GHz of $3\nu_2 + \nu_6$ compared to 10 GHz of $3\nu_2$,¹¹ is considerably greater than that of the corresponding excitation by Anderson *et al.*¹ of ν_6 at $\nu_2 = 1$, where a 25% reduction in the linewidth has been observed (250 MHz vs 330 MHz). The band origin of the lowest component of $3\nu_2 + \nu_6$, $K = 1$, is $\nu_o = 11\,537.047(5)\text{ cm}^{-1}$. The displacement of the $3\nu_2 + \nu_6$ band origin from that of $3\nu_2$ yields $\nu_6 = 493.96(3)\text{ cm}^{-1}$ for the $K = 1$ level of the intermolecular out-of-plane bending frequency at $\nu_2 = 3$.

B. The $K = 0 \leftarrow 0$ Subband of $3\nu_1 + \nu_4$. The spectrum of the $K = 0 \leftarrow 0$ subband of $3\nu_1 + \nu_4$ is observed from $11\,405\text{ cm}^{-1}$ to $11\,398\text{ cm}^{-1}$. A portion of the action spectrum centered around $11\,402\text{ cm}^{-1}$ is shown in Figure 2. This band is a

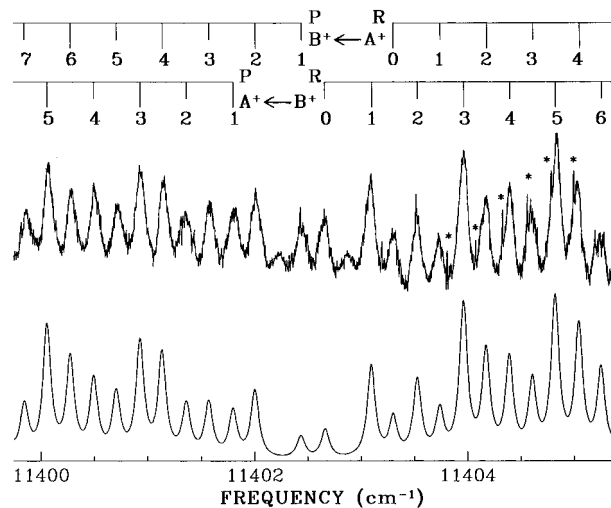


Figure 2. $K = 0 \leftarrow 0$ subband of the $3\nu_1 + \nu_4$ mode of $(\text{HF})_2$, taken under the same experimental conditions as Figure 1. The sharp spikes, labeled by asterisks, are the rovibrational lines of the Q branch of the ArHF(3111) \leftarrow (0100) hot band transition. The simulated spectrum shown underneath is generated by using a rotational temperature of 15 K, band origin of $11\,402.867\text{ cm}^{-1}$ ($11\,402.230\text{ cm}^{-1}$), rotational constant of $0.217\,04\text{ cm}^{-1}$ ($0.216\,39\text{ cm}^{-1}$), centrifugal constant of $2 \times 10^{-6}\text{ cm}^{-1}$, and Lorentzian width of 2.5 GHz for the $B^+ \leftarrow A^+$ ($A^+ \leftarrow B^+$) transition.

parallel $K = 0 \leftarrow 0$ transition, characterized by the absence of Q branches and the $4\bar{B}$ ($\approx 0.8\text{ cm}^{-1}$) gap between the R(0) and P(1) lines in the spectrum. The assignment of the rovibrational lines for the two tunneling states is verified by the intensity alternation in the transitions arising from even and odd J' . Due to the specific nuclear spin statistics, the weights for even:odd J' are 10:6 (6:10) for the transitions originating from the A^+ (B^+) level of the $K = 0$ ground vibrational state. Note also in Figure 2 that the sharp features, labeled by asterisks, are Q-branch lines of the ArHF (3111) \leftarrow (0100) hot band transition. The three-fold improvement in S/N as well as enhanced laser stability by the present AM scheme enable us to observe these intrinsically weak transitions.

The observed $K = 0 \leftarrow 0$ rovibrational lines are fitted with the standard polynomial expansion in $J(J + 1)$ for a very slightly asymmetric prolate top:

$$E_v(J) = \nu_0(v) + \bar{B}(v)J(J + 1) - D(v)[J(J + 1)]^2$$

where $\bar{B} = (B + C)/2$. By fixing the ground-state term values to those determined from microwave measurements,¹ the molecular constants at $v = 3$ can readily be obtained. The fitted constants and calculated term values of the two tunneling components are listed in Table 1, from which we obtained $\nu_0 = 11\,402.889(4)\text{ cm}^{-1}$ and $\bar{B} = 0.216\,39(17)\text{ cm}^{-1}$ for component A^+ and $\nu_0 = 11\,402.868(8)\text{ cm}^{-1}$ and $\bar{B} = 0.217\,04(84)\text{ cm}^{-1}$ for component B^+ , respectively, with both D' and D'' constrained to $2 \times 10^{-6}\text{ cm}^{-1}$ in the fitting. The fitting is good to about $\pm 0.01\text{ cm}^{-1}$, as expected from a linewidth of 0.09 cm^{-1} and a S/N ≈ 10 . Note that the upper state, B^+ , is 0.021 cm^{-1} lower than A^+ , which is equivalent to a tunneling splitting of $\Delta_{vt} = \nu_0(B^+) - \nu_0(A^+) = -0.021(8)\text{ cm}^{-1}$ for the $3\nu_1 + \nu_4$ state. This can be compared to the corresponding values of 19.747 24 GHz ($0.658\,69\text{ cm}^{-1}$) for the ground state¹ and -49.92 GHz (-1.664 cm^{-1}) for $K = 0$ of $\nu_1 + \nu_4$.¹ The origin of this band is blue-shifted from that of the pure overtone state $3\nu_1$ at $11\,273.501\text{ cm}^{-1}$ by 129.367 cm^{-1} .

The widths of the rovibrational lines shown in Figure 2 are determined by fitting to Voigt profiles with the constrained

TABLE 1: Observed Term Values and Fitted Molecular Constants (in cm⁻¹) of the 3ν₁ + ν₄ K = 0 Subband of (HF)₂^a

<i>J</i>	<i>E</i> (<i>J</i> ,A ⁺)	<i>E</i> (<i>J</i> ,B ⁺)
0	11 402.893(4)	11 402.870(2)
1	11 403.313(-8)	11 403.306(4)
2	11 404.186(-1)	11 404.175(5)
3	11 405.493(8)	11 405.465(-7)
4	11 407.216(0)	11 407.220(12)
5	11 409.378(0)	11 409.390(13)
6	11 411.983(10)	11 411.990(10)
7	11 414.988(-13)	11 415.024(8)
<i>v</i> ₀	11 402.889(4)	11 402.868(8)
<i>B</i>	0.216 39(17)	0.217 04(15)

^a The standard deviation in frequency measurements is ±0.007 cm⁻¹. Numbers in parentheses are deviations (the observed minus the calculated) in unit of the last digit.

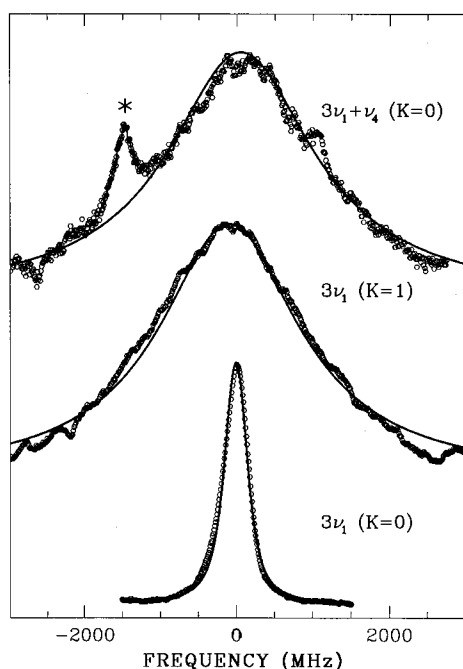


Figure 3. Comparison of the typical line shapes of the 3ν₁ (*K* = 0), 3ν₁ (*K* = 1), and 3ν₁ + ν₄ (*K* = 0) subbands of (HF)₂. The circles are the experimental data fitted to Voigt profiles with a Doppler width of 180 MHz. The Lorentzian components, from vibrational predissociation, are determined to be 240(10) MHz for 3ν₁ (*K* = 0), 2.1(2) GHz for 3ν₁ (*K* = 1), and 2.5(2) GHz for 3ν₁ + ν₄ (*K* = 0). The sharp feature (labeled by an asterisk), overlapped with the 3ν₁ + ν₄ (*K* = 0) line, is the Q(3) of ArHF(3111) ← (0100).

Doppler width of 180(10) MHz as stated earlier. The typical result of the fitting is presented in Figure 3. The linewidths do not vary appreciably with rotational level and are independent of tunneling state. In contrast to the sharpness of the pure 3ν₁ *K* = 0 mode, the Lorentzian width of the 3ν₁ + ν₄ *K* = 0 mode is 2.5(2) GHz, which is an order of magnitude larger than that of the pure 3ν₁ overtone state. A typical line from the 3ν₁ *K* = 1 subband is also shown with a fitted Lorentzian component of 2.1(2) GHz, in excellent agreement with earlier measurement.¹¹

Discussion

A. Band Assignments. We assign the features at 11 402 cm⁻¹ to 3ν₁ + ν₄, the combination mode of the second overtone free HF stretch (3ν₁) with the intermolecular F–F stretch (ν₄). The assignment is based on the energy difference of 3ν₁ + ν₄ – 3ν₁ = 129.368 cm⁻¹,¹¹ which is quite similar to ν₁ + ν₄ – ν₁ = 127.573 cm⁻¹ at the fundamental. The average rotational

constant of the states A⁺ and B⁺ is 0.2167 cm⁻¹, appreciably smaller than 0.221 18 cm⁻¹ of the 3ν₁ state.¹¹ Such an elongation of the heavy atom distance is expected upon excitation of the hydrogen bond stretching. The 2% reduction in rotational constants observed at 3ν₁ + ν₄ is similar to that at ν₁ + ν₄.¹ Hence, there is little reason to question this assignment.

Since ν₄ is the heavy atom or hydrogen bond stretching motion, it might at first sight be expected that *n*ν₁ + ν₄ – *n*ν₁ should be sensibly independent of the valence excitation or, equivalently, the bond lengthening of the free HF, the proton acceptor. This, however, is far from obvious. Our previous studies¹¹ showed that the *B* rotational constant of the 3ν₁ level has increased by 2% from the value at the ground vibrational level. It is likely that most of this increase is a consequence of the change of α, the angle between the free-HF internuclear axis and the F–F line. From the large reduction (26%) in the *A* rotational constant,¹¹ the value of α has increased markedly upon valence vibrational excitation. The constancy of the frequency of the intermolecular stretching motion with ν₁ thus implies minor dependence of the hydrogen bond vibration upon ν₁ excitation or, equivalently, the bond lengthening of the free HF.

We consider now the vibrational assignment of the band at 11 537 cm⁻¹, which had been assigned, previously, as (ν₁,ν₂) = (1,2).¹² That assignment was based on the assumption that the four fundamental members of the *N* = 3 vibrational polyad would have the highest intensity in the 11 000–11 500 cm⁻¹ spectral region. There have been few guides for vibrational intensities of the hydrogen fluoride dimer. We may note that in the one theoretical effort¹⁹ that did consider overtone vibrational intensities of this system, the predicted intensity ratios within the *N* = 3 polyad scaled as (3,0):(2,1):(1,2):(0,3) = 1.12:0.09:0.39:0.12. Thus it appeared likely that all members would have similar observability and there was little reason to exclude any member of the polyad based on the predicted intensities.

Discrimination between the four bands is possible by employing different detectors which are sensitive in specific energy ranges. The virtue of the energy-specific detector in vibrational laser induced fluorescence is that it allows some identification of product vibrational states. In a sense it is the simplest (and crudest) scheme for analysis of the fluorescence radiation. In particular, upon excitation of the *N* = 3 polyad of (HF)₂, the product HF should have *N*_p = 2, where *N*_p = ν_a + ν_b with *a* and *b* denoting the two HF photofragments. We have noted that the longest predissociation time for *N* = 3 is 0.66 ns; thus all of the fluorescence observed is from HF photofragments. The lead sulfide detector, having sensitivity to radiation with energy greater than 3300 cm⁻¹, will always detect the excitation process since both HF(ν=2) and HF(ν=1) will emit radiation in this region. The germanium detector, however, provides photoproduct selectivity since it only detects radiation with energy greater than 6400 cm⁻¹. This requires at least one dissociation pathway leading to the production of HF(ν=2) for detection.

It appears quite reasonable physically to argue that the dissociation pathway of the *N* = 3 polyad (ν₁,ν₂) is dominated by



The pathway is simply stated as a unit loss of a vibrational quantum from the proton donor unit, except for (3,0). We have labeled the product HF units with *a* and *b*, since Miller and co-workers²⁰ have shown for the $N = 1$ fundamental dyad that the free HF subunit correlates to a low-rotation product, while the bonded HF constitutes a highly rotationally excited product. It is clear that the expected vibrational predissociation pathway of (HF)₂ at $\nu_1 + 2\nu_2$ is to 2HF($\nu=1$), since the hydrogen-bonded proton-donating unit is known to show a more efficient vibrational predissociation.^{21–23} On the basis of this vibrational product analysis, the 11 537 cm⁻¹ band, which is readily observed by using the germanium detector, should not be assigned as originating from the $\nu_1 + 2\nu_2$ state. It is therefore highly likely that our earlier band assignment¹² was incorrect. The more appropriate assignment of this band is $K = 1$ of $3\nu_2 + \nu_6$.

Recently Anderson et al. presented a valuable, extensive study of the combination bands of the hydrogen fluoride dimer at the fundamental valence vibration. Of particular importance here is the combination band, $\nu_2 + \nu_6$. They observed only a $K = 1 \leftarrow 0$ feature of this combination mode in absorption for both (HF)₂ and (DF)₂ from their slit-jet-cooled systems.^{1,24} The ν_6 , $K = 1$ feature for (HF)₂ is displaced 425.690 cm⁻¹ from the band origin of ν_2 , $K = 0$. Under the present reassignment of the 11 537 cm⁻¹ band to $3\nu_2 + \nu_6$, the displacement of ν_6 $K = 1$ from $3\nu_2$ is 493.9 cm⁻¹.¹¹ This assignment requires a strong dependence of ν_6 upon ν_2 excitation; the frequency increases slightly nonlinearly from 399.787 cm⁻¹ of $\nu_2 = 0$ (ref 25), 425.690 cm⁻¹ of $\nu_2 = 1$ to 493.96 cm⁻¹ of $\nu_2 = 3$. The best fit of these data yields $\nu_6(\nu_2) = 399.79 + 23.17\nu_2 + 2.734\nu_2^2 = 399.79(1 + 0.05796\nu_2 + 0.006839\nu_2^2)$, for the $K = 1$ series. We note that a large frequency increase in intermolecular modes upon valence excitation is not unusual in hydrogen bonded complexes. In the well-studied ArHF species, the analogous Π bending series²⁶ (ν_110) – (ν_000) can also be fitted⁴ by the quadratic form $64.925 + 4.685\nu + 0.445\nu^2 = 64.925(1 + 0.07216\nu + 0.00685\nu^2)$. Roughly these two systems differ in bending frequency and cross anharmonic constants by a factor of 6.

The present reassignment invites a more extensive search for the missing $\nu_1 + 2\nu_2$ band. The other three members of the $N = 3$ quartet have all been found. Our phenomenological model proposed earlier¹⁵ for the hydrogen interchange tunneling suggested that the band should be centered near 11 480 cm⁻¹, accompanied by a large tunneling splitting of $\Delta\nu_1 = +0.39$ cm⁻¹, essentially identical to the tunnel splitting of the $2\nu_1 + \nu_2$ band. The model relied upon a modest mechanical coupling of the local high-frequency oscillators within the hydrogen fluoride dimer. That the local oscillators are coupled is essentially the basis for V–V energy transfer in hydrogen fluoride collisions⁶ of the type HF(ν) + HF(0) \leftrightarrow HF($\nu-1$) + HF(1). Previously¹² we have extensively searched the predicted region using the lead sulfide detector but found no notable features that could be assigned to the HF dimer. This failure in detection could come from the same origin as the unobservability of the pure $2\nu_2$ band²⁷ due to lifetime broadening by rapid vibrational predissociation. A reasonable expectation for the upper limit of the linewidth of this band is 10 GHz, which is that of $3\nu_2$. From our previous estimation of band intensities,¹² the unobservability suggests that the $\nu_1 + 2\nu_2$ combination band has an absorption intensity at least 1 order of magnitude smaller than $3\nu_1$ or $3\nu_2$. Improvement of detection sensitivity and/or extensive signal averaging appears to be a requirement for observation of this exceedingly weak transition.

We point out that the three features $3\nu_1$, $3\nu_2$, and $2\nu_1 + \nu_2$ as well as several soft mode combination bands built upon these are readily observed by their $\Delta\nu = -2$ emission, since all are readily detected by using the high-energy germanium detector. This establishes that the predominant dissociation process in vibrational predissociation of (HF)₂ indeed is $\Delta N = 1$ at $N = 3$. We note that the linewidth for the $3\nu_2$ band is around 10 GHz, which is 30 times as large as the 0.33 GHz observed at the fundamental ν_2 vibration. The scaling is $\Gamma(n\nu_2)/\Gamma(\nu_2) = n^3$. The origin of this rapid increase in predissociation rate cannot be *directly* due to the obvious increase in level density, since the dissociation is dominated by the $\Delta N = 1$ channel. Thus the *effective* level density is sensibly independent of N . This phenomenon appears to be general; for example, in N₂HF the predissociation linewidth scales as ν^4 . Furthermore, it appears that the complexity of the dipole spectra is relatively similar at $N = 3$ to that at $N = 1$. This feature of similarity is common in a number of complexes of hydrogen fluoride for which comparisons have been made.⁴ It is, however, quite different from that commonly observed in valence-bonded systems.

It is characteristic of hydrogen fluoride complexes that a considerable reduction in predissociation rate occurs upon excitation of bending motions. The $n\nu_2$ excitation of (HF)₂ shows this clearly. At $n = 1$, excitation of ν_6 produces a 25% reduction in the predissociation rate¹. In the present work at $n = 3$, excitation of ν_6 results in a factor of 3 decrease. We note that in N₂HF at $\nu = 3$ there is an almost similar reduction upon Π bending excitation of 580 to 240 MHz. It appears that the very facile predissociation observed in the $\nu = 3$ level shows a greater reduction upon concurrent excitation of the bending of the HF unit than at $\nu = 1$.

B. Changes in Potential Energy Surface upon Valence Excitation. The frequency of the ($n\nu_1 + \nu_4$) – $n\nu_1$ series now exists for $n = 1$ (127.5762 cm⁻¹) and $n = 3$ (129.368 cm⁻¹). Under the assumption of a linear variation with ν_1 valence excitation, the extrapolated value at the ground state is 126.7 cm⁻¹ for the A⁺ component. This value is in excellent agreement with the value of 126.4 cm⁻¹ from the dynamical calculations of Zhang *et al.*⁵ Since the tunneling splitting in the $n\nu_1 + \nu_4$ series varies quite significantly with n , extrapolations to $n = 0$ are likely to contain appreciable uncertainties (± 0.5 cm⁻¹). For instance, if the extrapolation is instead done by using the *average* of the two tunneling doublets for each n , the extrapolated value at $n = 0$ is 127.7 cm⁻¹, which may be compared to the calculated 126.6 cm⁻¹ for the average. The origin of this discrepancy is the large doubling of 1.664 cm⁻¹ at $\nu_1 + \nu_4$. Table 2 gives the presently measured tunneling splittings at $n = 1$ and 3. As noted, the magnitude and sign of the doublings vary quite considerably among the four states at $N = 1$. It appears useful to attempt some elementary modeling to account for the large doubling as well as the enhanced predissociation observed at these $n\nu_1 + \nu_4$ levels.

Our modeling of the $n\nu_1 + \nu_4$ levels follows closely the phenomenological model set out earlier¹⁵ for the dependence of hydrogen interchange tunneling upon valence excitation. We assume a minimal set of interacting levels and attempt to fit tunneling splittings as well as predissociation linewidths. The predissociation rate of a state in which only ν_2 is excited is taken as a phenomenological parameter. The rate of predissociation of a state with ν_1 excitation is determined by the extent of mixing with ν_2 . In particular, we consider that the valence excitations of ν_1 and ν_2 are mechanically coupled, thus corrupting the pure local mode description. The magnitude and sign of the coupling constant, as well as its dependence upon

TABLE 2: Comparison of Hydrogen Interchange Tunneling Splittings (in cm⁻¹) and Vibrational Predissociation Broadenings (in MHz) between Measurements and Calculations of (HF)₂ at K = 0

mode	this model				observations ^a		
	ΔE_0^c	$\Delta\nu_0^b$	$\Delta\nu_t^d$	$\Delta\nu_{pd}^e$	$\Delta\nu_0^c$	$\Delta\nu_t^d$	$\Delta\nu_{pd}^f$
$\nu_1 + \nu_5$	33	46.76	-2.27	19 (A ⁺), 5 (B ⁺)	46.591	-2.739	20 (A ⁺), 45(B ⁺)
$\nu_1 + \nu_4$	15	4.57	-2.20	40 (A ⁺), 15 (B ⁺)	7.640	-1.664	25 (A ⁺), 40 (B ⁺)
$\nu_2 + \nu_5$	-11	-10.24	3.29		-4.090	3.587	270 (A ⁺ ,B ⁺)
$\nu_2 + \nu_4$	-37	-50.37	1.19		-50.141		300 (A ⁺ ,B ⁺)
$3\nu_1 + \nu_4$						-0.021	2500 (A ⁺ ,B ⁺)

^a Reference 1 and this work. ^b The frequencies are given in terms of the displacement from the average of the four states. ^c The input zero-order energies. ^d The tunneling splittings are defined as $\Delta\nu_t = \nu_0(\text{B}^+) - \nu_0(\text{A}^+)$. ^e The calculated predissociation linewidths are listed as the fractional composition of the ν_2 states times 300 MHz. ^f The vibrational predissociation broadenings of the two tunneling states, A⁺ and B⁺.

ν_1 and ν_2 , have previously been fitted.¹⁵ In the present modeling of the combination states, we also include the interaction between ν_4 and ν_5 (geared bend), since these two modes are quite close in frequency and are certainly coupled.¹ Finally we assume that the hydrogen interchange tunneling is more facile in $\nu_5 = 1$ than it is at $\nu_5 = 0$, since the coordinate of ν_5 is regarded as the tunnel path. These assumptions have essentially been made by many²⁸ who have examined the hydrogen fluoride dimer. The model then requires three new parameters. The tunneling splitting in the $\nu_5 = 1$ level is calculated by Zhang *et al.*⁵ as 7.48 cm⁻¹ and 0.44 cm⁻¹, for $\nu_5 = 0$. [Their notation ($\nu_3\nu_4\nu_5\nu_6$)²⁹ is E(0030) - E(0020) for $\nu_5 = 1$.] The uncertainty in using the value 7.48 cm⁻¹ for the $\nu_5 = 1$ tunneling doubling is difficult for us to estimate. It appears unlikely that simple scaling by the ratio of the observed value at $\nu_5 = 0$ of 0.66 cm⁻¹ to the calculated 0.44 cm⁻¹ would produce a more realistic value for $\nu_5 = 1$. We adopt a value of $\Delta\nu_t = 8$ cm⁻¹ at $\nu_5 = 1$. The tunneling splitting in our uncoupled $\nu_4 = 1$ is taken to be identical to that of the ground state, namely, 0.66 cm⁻¹.¹ Physically this would appear to be a reasonable one-dimensional picture since ν_4 is the intermolecular stretching vibration, a motion that is quite different than the angular motions associated with the donor-acceptor interchange. These choices have been discussed at length here since there are no experimental values at the ground valence excitation.

We model the ($\nu_1 + \nu_4$, $\nu_1 + \nu_5$, $\nu_2 + \nu_4$, $\nu_2 + \nu_5$) quartet with two (left and right) interchanged isoenergetic forms, giving an 8 × 8 energy matrix. The ν_4 and ν_5 frequencies and the tunneling splittings of all the combination modes have been well determined by Anderson, Davis and Nesbitt.¹ Table 2 presents a comparison of this model with their results. In the modeling, we have chosen the interaction constant between ν_4 and ν_5 to be $\lambda_{4,5} = -20$ cm⁻¹. The interaction between ν_1 and ν_2 remains $\lambda_{1,2} = -11$ cm⁻¹.¹⁵ We also assume that there is a small coupling between $\nu_1 + \nu_4$ and $\nu_2 + \nu_5$ as well as between $\nu_1 + \nu_5$ and $\nu_2 + \nu_4$, $\lambda_{14,25} = \lambda_{15,24} = -2$ cm⁻¹, due to soft mode-valence mode interactions. The other coupling elements are set to zero. The initial unperturbed frequencies are roughly adjusted to give the final frequency set. While the effort is clearly parametric and the results cannot be regarded as giving a quantitative fit, the qualitative trends of the tunneling splittings observed in the ($\nu_1 + \nu_4$, $\nu_1 + \nu_5$, $\nu_2 + \nu_4$, $\nu_2 + \nu_5$) quartet of (HF)₂ are reasonably matched. Note that the symmetry of the levels is properly given in Table 2. We have not attempted a refinement of the constants used as well as the input energies to optimize the tunneling splittings of the levels and their distribution, since the purpose of this modeling was to show that a reasonable choice of $\Delta\nu_t = 8$ cm⁻¹ for the “pure” ν_5 level allows reasonable estimates for the tunneling splittings of all members of the ($\nu_1 + \nu_4$, $\nu_1 + \nu_5$, $\nu_2 + \nu_4$, $\nu_2 + \nu_5$) quartet, without recourse to changes in the barrier with valence excitation.

Of considerable interest to us is the nature of the predissociation broadening of the levels associated with the ν_1 oscillations. We note that at both $N = 1$ and $N = 3$ for the pure overtone states, the ratio of predissociation rate of $n\nu_1$ to $n\nu_2$ is roughly 30–50. We have suggested previously¹⁵ that the predissociation of $\nu_1 = 1$ is predominantly due to the mechanical coupling of two idealized local mode oscillators in the actual spectroscopic states. The predissociation rate is then simply the fractional character of ν_2 in the state multiplied by the predissociation rate of ν_2 . In the present instance, we repeat these arguments and list the predicted predissociation rates of the four combination bands in Table 2. We find an appreciable difference between the tunnel pairs of the ν_1 component. The agreement between our calculations and the measurements of the Nesbitt group¹ are frankly disappointing for this quantity. These predictions of the predissociation are not sensitive to *minor* changes in the coupling constants.³⁰

It is worth comparing these results with the explicit calculations of Wu *et al.*⁵ using a 6D *ab initio* potential. These *ab initio* based calculations produce a smaller ratio for the tunneling doubling of ν_4 to ν_5 at $N = 1$ than our model. In all cases the signs of the doublings are in agreement. Their predissociation lifetimes, while different than our results, are similar in showing relatively poor agreement with the observed variations.

We have discussed at length the ν_4 and ν_5 levels at $N = 1$ to lay a foundation for the discussion of these soft mode oscillations at the $N = 3$ levels. In particular we wish to examine the large change in predissociation linewidths of $3\nu_1$ ($K = 1$) and $3\nu_1 + \nu_4$ ($K = 0$) due to interactions with nearby combination levels of $3\nu_2$, specifically $3\nu_2 + \nu_5$ ($K = 1$) and $3\nu_2 + \nu_4 + \nu_5$ ($K = 0$), respectively. A comparison of the linewidths of these bands with that of $3\nu_1$ ($K = 0$) is given in Figure 3. While the dependence of ν_5 upon the level of valence excitation is not yet determined, the dependence of ν_4 on ν_1 has been estimated earlier to be 2.7-cm⁻¹ blue shifted from $\nu_1 = 0$ to 3. We note that the shift of ν_4 upon ν_2 excitation is larger, since at $N = 1$ the difference is known¹ to be 5 cm⁻¹. Assuming a linear dependence of ν_4 on ν_2 , the observed frequencies of 126.7 cm⁻¹ at $\nu_2 = 0$ and 132.616 cm⁻¹ at $\nu_2 = 1$ provide the estimate $3\nu_2 + \nu_4 - 3\nu_2 = 143$ cm⁻¹. From the change in ν_5 of 19 cm⁻¹ at $\nu_2 = 1$, given by Nesbitt and co-workers,¹ linear extrapolation suggests $3\nu_2 + \nu_5 - 3\nu_2 = 216$ cm⁻¹, and thus $3\nu_2 + \nu_4 + \nu_5 = 11043 + 143 + 216 = 11402$ cm⁻¹. The difference in energies between $3\nu_1 + \nu_4$ ($K = 0$) observed at 11 402.9 cm⁻¹ and our above estimate of $3\nu_2 + \nu_4 + \nu_5$ ($K = 0$) is extremely small. Thus it is not surprising that the $3\nu_1 + \nu_4$ band is appreciably broadened relative to the 240 MHz linewidth of $3\nu_1$ ($K = 0$) because of this near-resonance coupling. Using the above estimate $3\nu_2 + \nu_5 - 3\nu_2 = 216$ cm⁻¹ places $3\nu_2 + \nu_5$ at 11259 cm⁻¹ compared to the observed location of $3\nu_1$ ($K = 0$) at 11 273.50 cm⁻¹. We assume that the coupling element between $3\nu_1$ and $3\nu_2 + \nu_5$ is identical to that between $3\nu_1 + \nu_4$

and $3\nu_2 + \nu_4 + \nu_5$ and also that the line broadening in $3\nu_1$ and $3\nu_1 + \nu_4$ are due solely to this mixing. Since a small shift of the location of $3\nu_2 + \nu_5$ is ignorable, we obtain the coupling element $[15(240/10000)]^{1/2} = 0.6 \text{ cm}^{-1}$. Using this value for the coupling element we determine the separation between $3\nu_1 + \nu_4$ and $3\nu_2 + \nu_4 + \nu_5$ to be 1.4 cm^{-1} , which is 0.5 cm^{-1} different from our previous estimate. These arguments can be applied to qualitatively account for the large difference in predissociation broadening ($\Delta\nu_{\text{pd}} = 2.1 \text{ GHz}$) of $3\nu_1$ ($K = 1$) relative to that of $K = 0$. We have previously¹¹ attributed this difference to the centrifugal interaction of $3\nu_1$ and $3\nu_2 + \nu_5$. In view of the energy mismatch of $3\nu_1 - 3\nu_2 + \nu_5 \approx 15 \text{ cm}^{-1}$, and the large A rotational constants ($\approx 27 \text{ cm}^{-1}$) of the two levels, their differences in A can contribute appreciably to the energy differences at $K = 1$. In particular the ν_5 oscillation is likely to increase the A rotational constant, bringing the $3\nu_1$ and $3\nu_2 + \nu_5$ $K = 1$ levels into closer register. We may note that at $\nu_2 = 1$ the difference in apparent A rotational constants of $\nu_2 + \nu_5$ and ν_1 is 30%.¹ In view of the likely increase in coupling matrix element between $3\nu_1$ and $3\nu_2 + \nu_5$ in $K = 1$, as a consequence of centrifugal interaction, we fit the linewidths by adjusting the differences in the A rotational constants, using a 30% difference between A of $3\nu_1$ and $3\nu_2 + \nu_5$. The coupling element is required to be 1.2 cm^{-1} to fit the 2.1 GHz linewidth of $3\nu_1$ ($K = 1$). Finally, we do not attempt here to calculate the small tunneling doublings of $3\nu_1$ ($\Delta\nu_t = -0.072 \text{ GHz}$) and $3\nu_1 + \nu_4$ ($\Delta\nu_t = -0.63 \text{ GHz}$), with the model discussed above for $N = 1$. It is likely that the $N = 3$ quartet together with their ν_4 and ν_5 combinations, a total of 24 states, should be included in such a treatment.

Conclusion

The experimental evidence for the present reassignment is the detection of laser-induced fluorescence of the $11\,537 \text{ cm}^{-1}$ band by the $\Delta\nu = 2 \rightarrow 0$ emission of the HF fragments. The use of specific vibrational product state production for the assignment of the quantum numbers of a multiplet, we believe, is new. The demonstration that in the $N = 3$ multiplet vibrational predissociation proceeds by $\Delta N = -1$ establishes that the large increase in predissociation rate is not a direct consequence of the increase in density of states. Detecting high-frequency overtone emission by using high-sensitivity infrared detectors also allows other weak combination modes, such as $3\nu_1 + \nu_4$, to be observed. The observation is important since low-frequency intermolecular modes are directly associated with the intermolecular potential energy surfaces, which is partially modified by valence excitations. The present reassignment of the $11\,537 \text{ cm}^{-1}$ subband to $3\nu_2 + \nu_6$ $K = 1$ (rather than $\nu_1 + 2\nu_2$) removes the largest discord of the simple weakly coupled oscillator model¹⁵ previously found at $N = 3$. The vibrational predissociation rate of the level $3\nu_2 + \nu_6$ is a factor of 3 slower than observed at $3\nu_2$, in contrast to the change observed for $\nu_2 + \nu_6$ where the reduction in rate from ν_2 is 25%. The increasing set of measurements at $N = 3$ allow valuable comparisons to the large data base established at the fundamental.¹ These hopefully will stimulate further *ab initio* calculations at large displacements of the valence coordinates. This should enable additional rigorous tests for the advanced *ab initio* calculations,^{5,28} which have been actively performed recently, as well as extending our understanding of vibrational predissociation.

Acknowledgment. We thank the National Science Foundation for the financial support of this research. We are indebted to Dr. Peter Schulz for essential aid. We thank Mr. Harvey Smith

for assistance throughout this research. We thank Prof. Robert Field for valuable criticism of this manuscript.

References and Notes

- (1) See, for example: Anderson, D. T.; Davis, S.; Nesbitt, D. J. *J. Chem. Phys.* **1996**, *104*, 6225; **1996**, *105*, 4488, which provide excellent discussions and references for the $(\text{HF})_2$ complex.
- (2) Nesbitt, D. J. *Faraday Discuss. Chem. Soc.* **1994**, *97*, 1.
- (3) Miller, R. E. *Acc. Chem. Res.* **1990**, *23*, 10.
- (4) Chang, H.-C.; Klemperer, W. *Faraday Discuss. Chem. Soc.* **1994**, *97*, 95.
- (5) Zhang, D. H.; Wu, Q.; Zhang, J. Z. H.; von Dirke, M.; Bacic, Z.; *J. Chem. Phys.* **1995**, *102*, 2315. Wu, Q.; Zhang, D. H.; Zhang, J. Z. H. *Ibid.* **1995**, *103*, 2548 and references therein.
- (6) See, the recent review of: Flynn, G. W.; Parmenter, C. S.; Wodtke, A. M. *J. Phys. Chem.* **1996**, *100*, 12817, where a considerable discussion of the HF system is given.
- (7) Bemish, R. J.; Bohac, E. J.; Wu, M.; Miller, R. E. *J. Chem. Phys.* **1994**, *101*, 9457.
- (8) Lovejoy, C. M.; Nesbitt, D. J. *J. Chem. Phys.* **1987**, *86*, 3151.
- (9) Farrell, Jr., J. T.; Sneh, O.; Nesbitt, D. J. *J. Chem. Phys.* **1994**, *98*, 6068.
- (10) Tsang, S. N.; Chang, H.-C.; Klemperer, W. *J. Phys. Chem.* **1994**, *98*, 7313; Tsang, S. N.; Chuang, C.-C.; Mollaaghababa, R.; Klemperer, W.; Chang, H.-C. *J. Chem. Phys.* **1996**, *105*, 4385.
- (11) Chang, H.-C.; Klemperer, W. *J. Chem. Phys.* **1993**, *98*, 9266.
- (12) Chang, H.-C.; Klemperer, W. *J. Chem. Phys.* **1994**, *100*, 1.
- (13) The Lorentzian component of 100 MHz previously reported¹¹ was the half-width at half-maximum.
- (14) Chang, H.-C.; Klemperer, W. *J. Chem. Phys.* **1993**, *98*, 2497.
- (15) Chang, H.-C.; Klemperer, W. *J. Chem. Phys.* **1996**, *104*, 7830.
- (16) Schulz, P., private communication.
- (17) This work is aided in part by the Philips Laboratory and the Air Force Office of Scientific Research under Task 2303EPI/PL007.
- (18) Pugh L. A.; Rao, K. N. in *Molecular Spectroscopy: Modern Research*; Rao, K. N., Eds.; Academic Press: New York, 1976, Vol. II, Chapter 4, p 165.
- (19) Jensen, P.; Bunker, P. R.; Karpfen, A.; Kofranek, M.; Lischka, H. *J. Chem. Phys.* **1990**, *93*, 6266. Bunker, P. R.; Jensen, P.; Karpfen, A. *J. Mol. Spectrosc.* **1991**, *149*, 512.
- (20) Bohac, E. J.; Marshall, M. D.; Miller, R. E. *J. Chem. Phys.* **1992**, *96*, 6681; Marshall, M. D.; Bohac, E. J.; Miller, R. E. *Ibid.* **1992**, *97*, 3307 and references therein.
- (21) Huang, Z. S.; Jucks, K. W.; Miller, R. E. *J. Chem. Phys.* **1985**, *85*, 3338.
- (22) Pine, A. S.; Lafferty, W. J.; Howard, B. J. *J. Chem. Phys.* **1984**, *81*, 2939.
- (23) Pine, A. S.; Fraser, G. T. *J. Chem. Phys.* **1988**, *89*, 6636.
- (24) Davis, S.; Anderson, D. T.; Nesbitt, D. J. *J. Chem. Phys.* **1996**, *105*, 6645.
- (25) von Puttkamer, K.; Quack, M.; Suhm, M. A. *Mol. Phys.* **1988**, *65*, 1025.
- (26) The states of ArHF are designated by the label $(vbKn)$, where v denotes the HF valence stretching quantum number, b the bending quantum number, K the projection of rotational angular momentum on the molecular axis, and n the van der Waals stretching quantum number.
- (27) Suhm, M. A.; Farrell, Jr., J. T.; McIlroy, A.; Nesbitt, D. J. *J. Chem. Phys.* **1992**, *97*, 5341.
- (28) See, for example, the recent publications of Quack, M.; Suhm, M. A. *Chem. Phys. Lett.* **1995**, *234*, 71. Klopfer, W. Quack, M.; Suhm, M. A. *Chem. Phys. Lett.* **1996**, *261*, 35. W. Peterson, K. A.; Dunning, T. H. *J. Chem. Phys.* **1995**, *102*, 2032. Collins, C. L.; Horihashi, K.; Yamaguchi, Y.; Schaefer, H. F. *J. Chem. Phys.* **1995**, *103*, 6051. Necochea, W. C.; Truhlar, D. G. *Chem. Phys. Lett.* **1996**, *248*, 182.
- (29) Marshall, M. D.; Jensen, P.; Bunker, P. R. *Chem. Phys. Lett.* **1991**, *176*, 255.
- (30) We have applied the same model to $(\text{DF})_2$. We did not vary the coupling constants other than by the overall scaling with square root of reduced mass. Since the coordinate of ν_5 has been assumed to be the tunnel path, we also put an enhanced tunneling doubling in that vibrationally excited state. The $(\text{DF})_2$ tunneling splittings measured by Davis *et al.*,²⁴ however, show little correlation with our calculations other than in overall magnitude. In particular, the observed result that the relatively well isolated state $\nu_1 + \nu_4$ has a large tunneling doubling is not readily explained. The predictions of predissociation exhibit minor variation within the ν_1 vibrational manifold, in accord with observations.